

Cite this: *Chem. Sci.*, 2021, **12**, 14309

All publication charges for this article have been paid for by the Royal Society of Chemistry

Received 21st August 2021
Accepted 8th October 2021

DOI: 10.1039/d1sc04647k
rsc.li/chemical-science

Introduction

Magnetic resonance imaging (MRI) provides an attractive non-invasive imaging method to determine structure and function with high spatial and temporal resolution. MRI has the ability to detect and monitor complex molecular systems for chemical and biochemical analysis by relying on nuclear magnetic resonance (NMR). However, its widespread applicability is limited by the inherently low sensitivity of magnetic resonance at thermal equilibrium. The hyperpolarization technique, by inducing non-equilibrium polarization, can enhance NMR signal by several orders of magnitude and has been applied successfully to increase MRI sensitivity. Hyperpolarization of heteronuclei (e.g., ^{13}C and ^{15}N) is particularly useful, as real-time *in vivo* detection of these heteronuclei allows for investigating many dynamic metabolic and physiologic processes that were previously inaccessible to imaging.¹ The observable time window of a hyperpolarized molecule is primarily governed by the spin-lattice relaxation time (T_1) of the nucleus within the molecules of interest. Nuclei in certain functional groups, such as ^{13}C -carboxylic acids or quaternary ^{15}N -amine salts, have been found to have relatively long T_1 due to reduced dipole-dipole interaction without attached protons.² The comparably long-lived properties lead to a relatively slow signal decay

amenable for investigating slow processes, thus allowing translation into clinic practice.³

However, it is challenging to achieve long-lived ^{13}C or ^{15}N centers in a target molecule that lacks a ^{13}C -carbonyl group or quaternary ^{15}N -amine motif. For many biologically important molecules,⁴ the practicality of the corresponding isotopomers is limited by their short T_1 lifetimes. A short detection time window for hyperpolarized molecules presents challenges for developing effective HP-MRI agents for biomedical and clinical applications. A novel strategy to address this limitation is to incorporate a molecular tag that is capable of supporting long-lived hyperpolarization into target molecules. We have recently reported the development of $^{15}\text{N}_2$ -diazirines⁵ and $^{15}\text{N}_4$ -1,2,4,5-tetrazines⁶ as molecular tags for hyperpolarized NMR and MRI applications. Herein, we report that ^{15}N -labeled-azide constitutes a novel class of hyperpolarized molecular tag, offering superior practicality and efficacy as well as potentially broader imaging applications (Fig. 1).

We envisioned that the $(^{15}\text{N})_3$ -azide group, absent of directly attached protons, is theoretically capable of affording long-lived hyperpolarization. Furthermore, the three distinct nitrogen atoms of the azide will each provide a discrete chemical shift peak on ^{15}N -NMR that can be used for detection. Another attractive property of the azide group is that it fulfills many of the characteristics desirable in a molecular tag, featuring small size, unobtrusive electronic properties, stability in acidic or

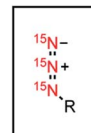
^aDepartment of Chemistry, Duke University, Durham, North Carolina, 27708, USA.
E-mail: warren.warren@duke.edu; qiu.wang@duke.edu

^bDepartment of Physics, Duke University, Durham, North Carolina, 27708, USA

^cDepartment of Radiology and Biomedical Engineering, Duke University, Durham, North Carolina, 27708, USA

† Electronic supplementary information (ESI) available: Synthesis of $(^{15}\text{N})_3$ -azide-tagged molecules, and (^{15}N) -azide-tagged molecules, hyperpolarization experiments, ^1H , ^{13}C and ^{15}N -NMR spectra as well as data analysis. See DOI: 10.1039/d1sc04647k

‡ These authors contributed equally to this work.



- long-lived hyperpolarized signals on ^{15}N centers
- three distinct ^{15}N chemical shifts for NMR detection
- azide known as the most commonly used chemical reporter with extensive examples of diverse biomolecules
- potential for multimodal imaging by bioorthogonal reaction

Fig. 1 $(^{15}\text{N})_3$ -Azide as a practical and effective tag for HP-MRI.

basic conditions, bioorthogonality, and synthetic ease of use.⁷ Numerous applications of the azides as a reaction partner in Staudinger reactions and azide–alkyne cycloaddition have been documented, representing a cornerstone in chemical biology and bioconjugation chemistry.^{7d,8} As the most commonly used chemical reporter, the azides have been used in the studies of nearly every class of biomolecules, including carbohydrates,⁹ amino acids,¹⁰ cholesterol,¹¹ nucleosides,¹² and lipids.¹³ Thus, the $(^{15}\text{N})_3$ -azide group, in addition to being a potential long-lived molecular tag for hyperpolarized NMR and MRI, can be used simultaneously in a bioorthogonal reaction to introduce other imaging readouts,^{7d,8,14} allowing for development of multimodal imaging agents.

In this paper, we investigated hyperpolarization of a series of $(^{15}\text{N})_3$ -azide-tagged molecules to examine the efficacy and potential of $(^{15}\text{N})_3$ -azides as a long-lasting hyperpolarized tag. We also evaluated the ability of single-labeled $(^{15}\text{N})(^{14}\text{N})_2$ -azide-tagged molecules as alternatives to offer long-lived hyperpolarization. The wide applicability and diverse examples of azide-labeled biomolecules exemplify the potentials of ^{15}N -labeled azides as novel and practical molecular tags for developing effective hyperpolarized agents in broad biomedical applications.

Results and discussion

Design and synthesis of $(^{15}\text{N})_3$ -tagged molecules

Our studies began with the design and synthesis of a series of compounds **1–6**, including choline, amino acids, glucoses, and an HIV drug azidothymidine (AZT) (Table 1). They were chosen as representative examples for diverse biologically important molecules that have the potential to be developed into hyperpolarized probes and to be pursued in future biomedical applications, such as understanding the metabolic basis of related diseases as well as drug pharmacology and mode of action.^{2b} First, sodium $(^{15}\text{N})_3$ -azide, the key reagent for the synthesis of all $(^{15}\text{N})_3$ -labeled compounds, was prepared by the oxidation of commercially available $(^{15}\text{N})_2$ -hydrazine monohydrate with ^{15}N -isoamyl nitrite.¹⁵ Next, $(^{15}\text{N})_3$ -azide-tagged molecules **1–6** were synthesized in 3–5 steps readily from commercially available reagents.¹⁶ The locations of $(^{15}\text{N})_3$ -azides in the biomolecules were strategically selected so the tags have minimal effect on the bioactivity of molecules. The rapid access to $(^{15}\text{N})_3$ -labeled compounds **1–6** highlights the easiness and efficiency of $(^{15}\text{N})_3$ -azide incorporation into target molecules, as well as its good compatibility with various functional groups,

Table 1 Enhancements (ε), polarization levels (P) and relaxation times (T_1) for $(^{15}\text{N})_3$ -azides **1–6** by d-DNP^a

Cmpd	Molecular structure 	T_1/min				
		ε	$P/\%$	$\text{N}\alpha$	$\text{N}\beta$	
1		336 700	11.6	(2.4 ± 0.2) $(0.36 \pm 0.03)^b$	(2.9 ± 0.2) $(0.10 \pm 0.01)^b$	(3.3 ± 0.2) $(0.25 \pm 0.02)^b$
2		254 900	8.8	(3.0 ± 0.2)	(4.0 ± 0.2)	(7.6 ± 0.3)
3		322 300	11.1	(3.0 ± 0.3)	(5.6 ± 0.3)	(8.1 ± 0.2)
4		142 500	4.9	(3.5 ± 0.3)	(6.2 ± 0.9)	(9.8 ± 1.7)
5		80 200	2.8	(1.9 ± 0.2)	(4.0 ± 0.3)	(6.8 ± 0.9)
6		196 800	6.8	(2.5 ± 0.1)	(3.6 ± 0.1)	(5.3 ± 0.1)

^a Each experiment repeated twice. Measurements performed at $B = 1$ T unless noted otherwise. Enhancements and polarization levels averaged over all ^{15}N sites. T_1 lifetimes derived by fitting the experimental data to a single exponential decay function and then compensating the effect of using the small flip angle pulses (see ESI for details). ^b T_1 lifetime measured at $B = 16.4$ T using thermally polarized **1** in D_2O .



allowing for the chemical labeling of $(^{15}\text{N})_3$ -azide in late stage of target molecule synthesis.

Hyperpolarization of $(^{15}\text{N})_3$ -azide-tagged molecules using d-DNP

To investigate hyperpolarization of these $(^{15}\text{N})_3$ -tagged molecules, we first determined the chemical shift assignments by ^{15}N spectroscopic analysis of thermally polarized $(^{15}\text{N})_3$ -azidocholine **1**, including its ^{15}N -NMR spectra with and without ^1H decoupling acquired at a magnetic field of 16.4 T (Fig. 2). Based on the J -coupling analysis of $J_{\text{N-N}}$ -couplings and $J_{\text{N-H}}$ -couplings as annotated in Fig. 2, the chemical shift assignments for $^{15}\text{N}\alpha$, $^{15}\text{N}\beta$, and $^{15}\text{N}\gamma$ were as follows: $^{15}\text{N}\alpha$ appears in the most upfield region (~ 65 ppm), $^{15}\text{N}\beta$ appears in the most downfield region (~ 242 ppm), and $^{15}\text{N}\gamma$ appears in between (~ 210 ppm). Because the $(^{15}\text{N})_3$ -azide tags in these structures are not directly adjacent to the sites of chemical changes that occur in endogenous metabolic processes, the hyperpolarized species may not necessarily generate ^{15}N NMR shift changes sufficient for chemical shift imaging (CSI) in their respective metabolic processes. Thus, in this study, we focus on establishing efficacy and adaptability of $(^{15}\text{N})_3$ -azide as a remarkable tag that offers favorable long-lived hyperpolarization, paving the way for biomedical applications.

With the chemical shift assignments of $^{15}\text{N}\alpha$, $^{15}\text{N}\beta$, and $^{15}\text{N}\gamma$ established, we examined hyperpolarization efficiency of $(^{15}\text{N})_3$ -

labeled compounds **1–6** using dissolution dynamic nuclear polarization (d-DNP). DNP is a hyperpolarization method routinely used in preclinical studies.^{2b,17} It is capable of polarizing almost any molecule of interest and typically uses deuterated water as the dissolution solvent, allowing for the analysis of the sample in an aqueous solution. Thus, effective hyperpolarization of $(^{15}\text{N})_3$ -azides by d-DNP will represent an important step toward *in vivo* biomedical applications. Table 1 summarizes the signal enhancement (ϵ) and relaxation times (T_1) of three individual ^{15}N -atoms ($^{15}\text{N}\alpha$, $^{15}\text{N}\beta$, and $^{15}\text{N}\gamma$) of these $(^{15}\text{N})_3$ -labeled compounds measured at 1 T. Fig. 3 depicts the comparison of T_1 relaxation times of $(^{15}\text{N})_3$ -azides **1–6** as well as the T_1 differences among the three individual ^{15}N atoms of the $(^{15}\text{N})_3$ -azides. As shown in Table 1, each of the $(^{15}\text{N})_3$ -azides **1–6** displayed highly effective ^{15}N signal enhancements up to over 300 000-fold and long ^{15}N relaxation lifetimes up to 9.8 min at 1 T.

Our hyperpolarization experiments began with $(^{15}\text{N})_3$ -labeled azidoethylcholine **1**. It has been shown that choline analogs, in which a methyl group is replaced with an alkyl chain of up to five carbon atoms in length, incorporate efficiently into phospholipids.¹⁸ For example, ^{14}N -azidoethylcholine has been demonstrated to faithfully mimic endogenous choline and can be efficiently incorporated into all classes of choline phospholipid for fluorescence imaging of phospholipids in cells.¹⁹ Studies on hyperpolarization of ^{15}N -choline demonstrated its

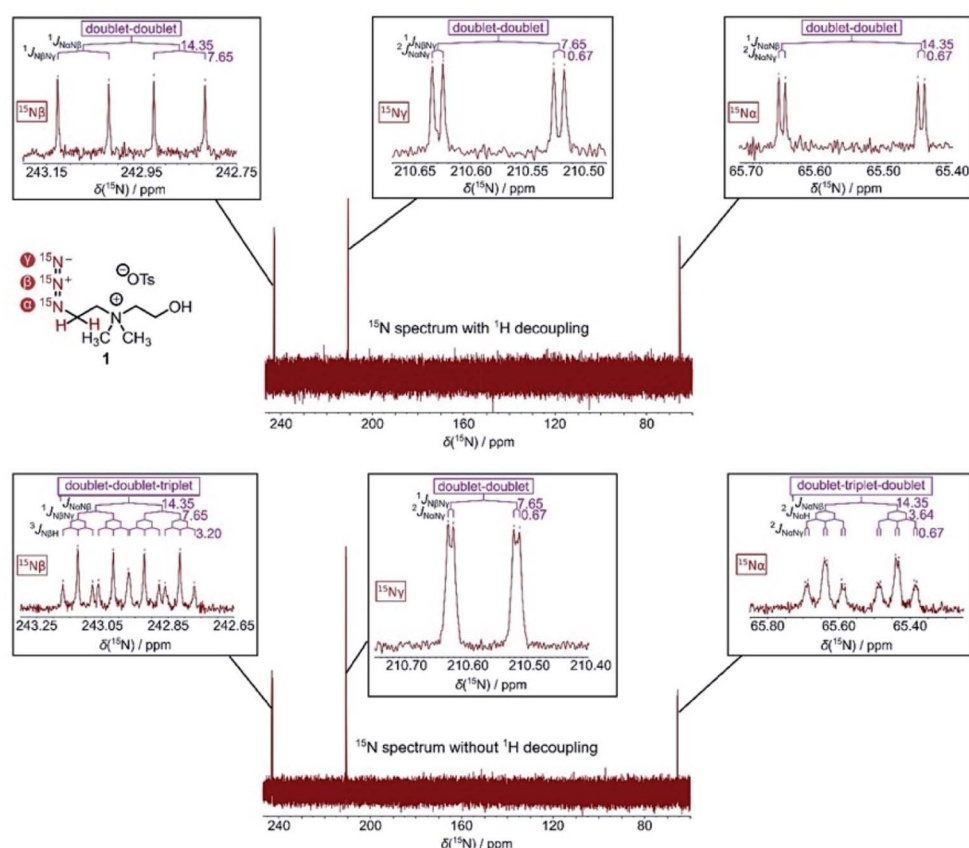


Fig. 2 ^{15}N -NMR spectra of thermally polarized $(^{15}\text{N})_3$ -azide **1** (253 mM in D_2O) acquired with (top) and without (bottom) ^1H decoupling. The ^{15}N spectra were measured at a magnetic field of 16.4 T.



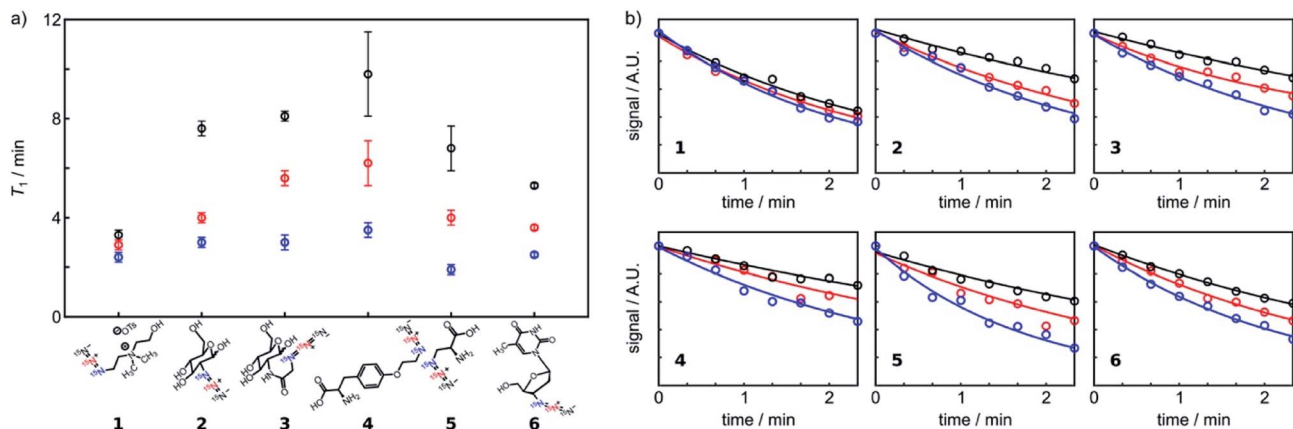


Fig. 3 (a) Comparison of T_1 relaxation times of $(^{15}\text{N})_3$ -azides (see Table 1 for T_1 values). (b) T_1 lifetime curves for $(^{15}\text{N})_3$ -azides. The experimental data points were fitted to an exponential decay function. The first 8 data points are shown.

use in imaging cellular choline uptake *in vitro* and *in vivo*.^{2a,20} Inspired by these earlier studies, we envision that $(^{15}\text{N})_3$ -azidoethylcholine **1** may serve as a potential HP-MRI probe to monitor elevated choline uptake leading to phospholipid metabolism. Hyperpolarization of $(^{15}\text{N})_3$ -azidoethylcholine analog **1** by d-DNP provided signal enhancement over 336 000-fold and T_1 value up to 3.3 min. The significantly enhanced and long-lived signals are highly encouraging for its *in vivo* imaging applications. Among the three different ^{15}N atoms of the $(^{15}\text{N})_3$ -azide, the terminal nitrogen ($^{15}\text{N}\gamma$) of the azide gave the longest T_1 lifetime, which results from the reduced dipole–dipole interaction in the absence of neighboring protons in comparison to $^{15}\text{N}\alpha$ and $^{15}\text{N}\beta$. The central $^{15}\text{N}\beta$ showed the second longest T_1 lifetime, followed by $^{15}\text{N}\alpha$ with the shortest T_1 due to the proximity to adjacent methylene protons. As shown in Table 1, T_1 lifetimes of thermally polarized $(^{15}\text{N})_3$ -azidocholine **1** were only 21.9 s for $^{15}\text{N}\alpha$, 6.0 s for $^{15}\text{N}\beta$ and 15.0 s for $^{15}\text{N}\gamma$ at a magnetic field of 16.4 T. The difference in ^{15}N T_1 lifetimes at different field strength is largely due to chemical shift anisotropy scaled linearly with B_0^2 , which suggests the advantage of imaging hyperpolarized azide tags at a low magnetic field.

We next evaluated hyperpolarization of $(^{15}\text{N})_3$ -azide-tagged glucose derivatives **2** and **3** (Table 1). ^{13}C -Labeled glucose has been developed for HP-MRI imaging of tumor glycolysis, yet it is limited by a narrow window of detection because of short polarization lifetime.²¹ In this study, we prepared $(^{15}\text{N})_3$ -labeled 2-azido-2-deoxy-glucose (2AzGlc) **2** and $(^{15}\text{N})_3$ -labeled azidoacetyl-glucosamine (GlcNAz) **3** as the representative analogs of $(^{15}\text{N})_3$ -azide-tagged monosaccharides. These two unnatural monosaccharide analogs, 2AzGlc and GlcNAz, have been reported as selective metabolic chemical reporters for glycosylation.²² Excitingly, d-DNP hyperpolarization of **2** and **3** provided ample ^{15}N -signal enhancement over 250 000-fold, and more importantly, the T_1 lifetime up to 8.1 min. The T_1 lifetimes observed on the $^{15}\text{N}\gamma$ atoms of **2** and **3**, benefiting from the reduced dipole–dipole interaction, are much longer (7.6 min and 8.1 min) than T_1 lifetimes observed on the $^{15}\text{N}\beta$ atoms (4 min and 5.6 min) and $^{15}\text{N}\alpha$ (3 min). Since a hyperpolarization experiment usually records signals for 5 times the T_1 relaxation

time, such long T_1 lifetime allows for data collection up to half an hour for $(^{15}\text{N})_3$ -azidoglucoses.

$(^{15}\text{N})_3$ -Azidotyrosine **4** and $(^{15}\text{N})_3$ -azidoalanine **5** have also been examined, as representative examples for $(^{15}\text{N})_3$ -azide incorporated amino acids that can be developed into hyperpolarized metabolic imaging probes. Hyperpolarization of $(^{15}\text{N})_3$ -azidotyrosine **4** by d-DNP afforded ^{15}N signal enhancement of \sim 142 000-fold and T_1 values of 3.5, 6.2 and 9.8 min for the $^{15}\text{N}\alpha$, $^{15}\text{N}\beta$, and $^{15}\text{N}\gamma$ positions, respectively. Hyperpolarization of $(^{15}\text{N})_3$ -azidoalanine **5** gave signal enhancement of \sim 80 000-fold and T_1 lifetime up to 6.8 min. In comparison with other $(^{15}\text{N})_3$ -azide-tagged compounds (*i.e.*, **1–3** and **6**), signal enhancements of **4** and **5** were largely affected by the acidity of the compounds.²³ Hyperpolarization of $(^{15}\text{N})_3$ -azidotyrosine **4** ($\varepsilon = \sim$ 142 000) and $(^{15}\text{N})_3$ -azidoalanine **5** ($\varepsilon = 80$ 000) was improved significantly by adding concentrated NaOH to neutralize a solution of their conjugate acids. The favorable polarization lifetime observed on $(^{15}\text{N})_3$ -azidotyrosine **4** and $(^{15}\text{N})_3$ -azidoalanine **5** suggested that the $(^{15}\text{N})_3$ -azido-tagging strategy offers an innovative platform, alternative to previous ^{15}N -labeled examples,²⁴ to design a diverse range of hyperpolarized amino acid imaging probes.

We also prepared and examined $(^{15}\text{N})_3$ -azidothymidine **6** to explore the applicability of $(^{15}\text{N})_3$ -azide tag on drug molecules for HP-MRI applications (Table 1). Azidothymidine (AZT), also known as Zidovudine, is an antiretroviral drug used for prevention and treatment of HIV/AIDS and contains an 3'-azide group in its structure.²⁵ Thus, $(^{15}\text{N})_3$ -AZT **6** would make an ideal exogenous probe for imaging HIV reverse transcriptase activity in addition to its therapeutic properties. Previous studies have shown that human cells uptake AZT rapidly within 100 seconds and AZT has low toxicity at high doses.²⁶ An earlier study determined polarization decay constants of $(^{15}\text{N})_2(^{14}\text{N})_2$ -AZT of 37 ± 2 s at 9.4 T and 140 ± 16 s at 50 mT for $\text{N}\gamma$.²⁷ In our study, hyperpolarization of $(^{15}\text{N})_3$ -AZT **6** by d-DNP provided signal enhancement over 196 000-fold and T_1 values up to 5.3 min at 1 T, reinforcing $^{15}\text{N}_3$ -AZT **6** a promising HP-MRI contrast agent for monitoring HIV progression and drug uptake.

Collectively, d-DNP hyperpolarization of $(^{15}\text{N})_3$ -azido compounds **1–6** all afforded high signal enhancement ($\varepsilon = 80\,000\text{--}336\,000$) and long-lived lifetimes (T_1 up to 9.8 min) at 1 T. Polarization levels up to 15% and hyperpolarization lifetimes of 3–4 min have been commonly observed for ^{15}N centers.⁵ We have deemed $(^{15}\text{N})_3$ T_1 lifetimes to be satisfactory for biological studies, as ^{13}C -isotopomers with T_1 of <1 min have been applied in *in vivo* imaging.⁴ Moreover, the large chemical shift dispersion among three ^{15}N atoms provides distinguishable ^{15}N signals that are well-suited for identification of species arising in the spectra. These examples highlight the efficiency and general adaptability of the $(^{15}\text{N})_3$ -azido as a hyperpolarized tag on endogenous biomolecules and exogenous drug molecules for broad biochemical or clinical applications.

Hyperpolarization of $(^{15}\text{N})(^{14}\text{N})_2$ -azide-tagged molecules using d-DNP

We next explored the potential of $(^{15}\text{N})(^{14}\text{N})_2$ -azide as an alternative hyperpolarized tag, considering the cost economic benefits of single ^{15}N -isotopically labeled azides and inspiring results that the terminal ^{15}N -atom of the azide group ($^{15}\text{N}\gamma$) consistently displayed the longest T_1 lifetimes in all $(^{15}\text{N})_3$ -azido compounds. The longer lifetime of $^{15}\text{N}\gamma$ was contributed by the reduced dipole–dipole interaction in the absence of neighboring protons in comparison to $^{15}\text{N}\alpha$ and $^{15}\text{N}\beta$.

We prepared three $(^{15}\text{N})(^{14}\text{N})_2$ -azide-tagged molecules, including (^{15}N) -azidoethylcholine **7**, (^{15}N) -azidoglucose derivative **8**, and (^{15}N) -AZT **9** (Table 2), as comparative studies with $(^{15}\text{N})_3$ -azido compounds **1**, **3**, and **6**. These (^{15}N) -azide-tagged molecules **7–9** were obtained as a mixture form of 1 : 1 ratio of $^{15}\text{N}\alpha$ - and $^{15}\text{N}\gamma$ -labeled azide. When (^{15}N) -azide-tagged molecules **7–9** were subjected to d-DNP hyperpolarization, we

used the signals measured at the $^{15}\text{N}\gamma$ sites for the enhancements and polarization levels, as signal to noise ratio were too low for the $\text{N}\alpha$ sites.²⁸ Excitingly, d-DNP-hyperpolarized (^{15}N) -azides **7–9** all afforded significantly enhanced and long-lived signals ($\varepsilon = 76\,000\text{--}121\,000$ and $T_1 = 3.2\text{--}7.6$ min, Table 2). These T_1 values are comparable to corresponding $^{15}\text{N}\gamma$ sites of $(^{15}\text{N})_3$ -azide analogs in Table 1. For example, hyperpolarized $(^{15}\text{N})(^{14}\text{N})_2$ -azide **7** displayed a T_1 lifetime of 3.2 min, analogous to 3.3 min measured at the $^{15}\text{N}\gamma$ atom of $(^{15}\text{N})_3$ -azidoethylcholine **1**. Similarly, T_1 lifetimes observed for hyperpolarized **8** ($T_1 = 7.6$ min) and **9** ($T_1 = 5.6$ min) were close to T_1 values of $(^{15}\text{N})_3$ -glucose **3** ($T_1 = 8.1$ min) and $(^{15}\text{N})_3$ -AZT **6** ($T_1 = 5.3$ min). These comparable long T_1 values observed on $(^{15}\text{N})_3$ - and $(^{15}\text{N})(^{14}\text{N})_2$ -azide-tagged compounds suggest that the relaxation resulting from ^{14}N -coupling has minimal effects in the solution phases. In comparison to the $(^{15}\text{N})_3$ -azido group, a single (^{15}N) -labeled azide offers one ^{15}N -peak for detection, yet it may function as an effective tag.

Hyperpolarization of $(^{15}\text{N})_3$ -azide-tagged molecules using SABRE-SHEATH

Finally, we examined the feasibility of hyperpolarization of $(^{15}\text{N})_3$ -azide-tagged molecules using an alternative hyperpolarization method, SABRE in SHield Enables Alignment Transfer to Heteronuclei (SABRE-SHEATH). Compared to d-DNP, SABRE-SHEATH is experimentally simple and cost-effective, yet its biomedical application is currently limited by poor performance in water. Subjecting $(^{15}\text{N})_3$ -azide **3** to SABRE-SHEATH in $\text{D}_4\text{-MeOH}$ provided enhanced and long-lived ^{15}N signals on all three individual $^{15}\text{N}\alpha$, $^{15}\text{N}\beta$, and $^{15}\text{N}\gamma$ atoms (Table 3). Compared to d-DNP hyperpolarization of $(^{15}\text{N})_3$ -azide **3** (Table 1), the SABRE-SHEATH hyperpolarization of $(^{15}\text{N})_3$ -azide **3**

Table 2 Enhancements (ε), polarization levels (P) and relaxation times (T_1) for $(^{15}\text{N})(^{14}\text{N})_2$ -azide **7–9** by d-DNP^a

Cmpd	Molecular structure	ε	$P/\%$	T_1/min		
				$\text{N}\alpha^b$	$\text{N}\beta$	$\text{N}\gamma$
7		76 000	2.6	—	—	(3.2 ± 0.3)
8		121 500	4.2	—	—	(7.6 ± 0.3)
9		28 600	1.0	—	—	(5.6 ± 0.6)

^a Each experiment repeated twice. Measurements performed at $B = 1$ T. Enhancements and polarization levels measured for $^{15}\text{N}\gamma$ sites. T_1 lifetimes derived by fitting the experimental data to a single exponential decay function and then compensating the effect of using the small flip angle pulses (see ESI for details). ^b Signal to noise ratio too low for $\text{N}\alpha$.



Table 3 Enhancements (ε), polarization levels (P) and relaxation times (T_1) for $(^{15}\text{N})_3$ -azide 3 by SABRE-SHEATH^a

	ε	$P/\%$	T_1/min
	$\text{N}\alpha$ 3060	0.11	(2.9 ± 0.9)
	$\text{N}\beta$ 27 600	0.95	(5.8 ± 0.1)
	$\text{N}\gamma$ 16 100	0.56	(9.2 ± 1.1)

3

^a Each experiment repeated twice by SABRE-SHEATH measured at 1 T. Detailed hyperpolarization conditions in ESI.

yielded lower polarization levels, with enhancement ranging from 3000- to 27 000-fold. Long T_1 lifetimes were observed, with T_1 value of 2.9 min on $^{15}\text{N}\alpha$, 5.8 min on $^{15}\text{N}\beta$, and 9.2 min on $^{15}\text{N}\gamma$. Note that the T_1 values observed for $(^{15}\text{N})_3$ -azide 3 in two experiments cannot be compared directly, considering the variants in solvents and radical/catalyst concentrations in d-DNP and SABRE-SHEATH experiments.

Overall, this is an initial attempt to hyperpolarize $(^{15}\text{N})_3$ -azide 3 by SABRE-SHEATH. The result is encouraging and demonstrate the ability of $(^{15}\text{N})_3$ -azide tag hyperpolarization using cost-efficient and convenient SABRE-SHEATH method. A systematic study on spin dynamics, the optimized experimental conditions for efficient polarization transfer, and the scope of the substrates using SABRE will be undertaken in future studies.

Conclusion

In summary, we have investigated the incorporation of $(^{15}\text{N})_3$ -azide as a general hyperpolarized molecular tag into biologically relevant molecules including choline, glucose, amino acids, as well as an antiretroviral drug. Hyperpolarization of $(^{15}\text{N})_3$ -azide-tagged molecules by d-DNP in water afforded enhanced detection sensitivity of ^{15}N signals up to six orders of magnitude. The three individual ^{15}N atoms of the $(^{15}\text{N})_3$ -azide displayed distinguishable ^{15}N chemical shifts and long-lasting hyperpolarization lifetimes. These favorable features of $(^{15}\text{N})_3$ -azide are well-suited as a practical and effective tag for developing novel HP-MRI agents. Furthermore, hyperpolarization of $(^{15}\text{N})_3$ -azide-tagged glucose derivative 3 has also been established using the experimentally simple and cost-effective SABRE-SHEATH method. Besides $(^{15}\text{N})_3$ -azide, a single $(^{15}\text{N})(^{14}\text{N})_2$ -labeled azido group is also found effective to function as a long-lived hyperpolarizable tag. Our future work will explore potentials of ^{15}N -azide tagged agents for broad *in vitro* and *in vivo* biomedical applications.

Author contributions

J. B. and H. P. conducted the synthesis and characterization of the compounds. G. Z. performed the hyperpolarization experiments. J. B. and Q. W. conceived and designed the project. W.

S. W. and Q. W. supervised the overall work. All authors participated in writing and editing the manuscript.

Conflicts of interest

There are no conflicts to declare.

Acknowledgements

This work was supported by NSF (CHE-1665090), NIH (R21EB024824), and the Camille and Henry Dreyfus Foundation. The content is solely the responsibility of the authors and does not necessarily represent the official views of the NIH. The authors thank Jacob R. Lindale and Shannon L. Eriksson for useful discussion on the derivation of the Hamiltonian of the spin system and analysis of the hydride spectrum.

References

- (a) J. H. Ardenkjær-Larsen, B. Fridlund, A. Gram, G. Hansson, L. Hansson, M. H. Lerche, R. Servin, M. Thaning and K. Golman, *Proc. Natl. Acad. Sci. U. S. A.*, 2003, **100**, 10158–10163; (b) K. Kumagai, K. Kawashima, M. Akakabe, M. Tsuda, T. Abe and M. Tsuda, *Tetrahedron*, 2013, **69**, 3896–3900; (c) W. Jiang, L. Lumata, W. Chen, S. R. Zhang, Z. Kovacs, A. D. Sherry and C. Khemtong, *Sci. Rep.*, 2015, **5**, 9104; (d) H. Nonaka, M. Hirano, Y. Imakura, Y. Takakusagi, K. Ichikawa and S. Sando, *Sci. Rep.*, 2017, **7**, 40104.
- (a) C. Gabellieri, S. Reynolds, A. Lavie, G. S. Payne, M. O. Leach and T. R. Ekyn, *J. Am. Chem. Soc.*, 2008, **130**, 4598–4599; (b) K. R. Keshari and D. M. Wilson, *Chem. Soc. Rev.*, 2014, **43**, 1627–1659.
- (a) K. M. Brindle, S. E. Bohndiek, F. A. Gallagher and M. I. Kettunen, *Magn. Reson. Med.*, 2011, **66**, 505–519; (b) E. M. Serrao and K. M. Brindle, *Front. Oncol.*, 2016, **6**, 59.
- S. Meier, M. Karlsson, P. R. Jensen, M. H. Lerche and J. Ø. Duus, *Mol. BioSyst.*, 2011, **7**, 2834–2836.
- (a) T. Theis, G. X. Ortiz, A. W. J. Logan, K. E. Claytor, Y. Feng, W. P. Huhn, V. Blum, S. J. Malcolmson, E. Y. Chekmenev, Q. Wang and W. S. Warren, *Sci. Adv.*, 2016, **2**, e1501438; (b) J. F. P. Colell, M. Emondts, A. W. J. Logan, K. Shen, J. Bae, R. V. Shchepin, G. X. Ortiz, Jr., P. Spannring, Q. Wang, S. J. Malcolmson, E. Y. Chekmenev, M. C. Feiters, F. Rutjes, B. Blumich, T. Theis and W. S. Warren, *J. Am. Chem. Soc.*, 2017, **139**, 7761–7767; (c) K. Shen, A. W. J. Logan, J. F. P. Colell, J. Bae, G. X. Ortiz Jr., T. Theis, W. S. Warren, S. J. Malcolmson and Q. Wang, *Angew. Chem., Int. Ed.*, 2017, **56**, 12112–12116; (d) H. Park, G. Zhang, J. Bae, T. Theis, W. Warren and Q. Wang, *Bioconjugate Chem.*, 2020, **31**, 537–541.
- J. N. Bae, Z. J. Zhou, T. Theis, W. S. Warren and Q. Wang, *Sci. Adv.*, 2018, **4**, eaar2978.
- (a) E. F. V. Scriven and K. Turnbull, *Chem. Rev.*, 1988, **88**, 297–368; (b) S. Brase, C. Gil, K. Knepper and V. Zimmermann, *Angew. Chem., Int. Ed.*, 2005, **44**, 5188–5240; (c) N. J. Agard, J. M. Baskin, J. A. Prescher, A. Lo and

C. R. Bertozzi, *ACS Chem. Biol.*, 2006, **1**, 644–648; (d) E. M. Sletten and C. R. Bertozzi, *Acc. Chem. Res.*, 2011, **44**, 666–676.

8 (a) C. I. Schilling, N. Jung, M. Biskup, U. Schepers and S. Bräse, *Chem. Soc. Rev.*, 2011, **40**, 4840–4871; (b) S. S. van Berkel, M. B. van Eldijk and J. C. M. van Hest, *Angew. Chem., Int. Ed.*, 2011, **50**, 8806–8827.

9 (a) E. Saxon and C. R. Bertozzi, *Science*, 2000, **287**, 2007–2010; (b) J. M. Baskin, J. A. Prescher, S. T. Laughlin, N. J. Agard, P. V. Chang, I. A. Miller, A. Lo, J. A. Codelli and C. R. Bertozzi, *Proc. Natl. Acad. Sci. U. S. A.*, 2007, **104**, 16793–16797.

10 (a) K. L. Kiick, E. Saxon, D. A. Tirrell and C. R. Bertozzi, *Proc. Natl. Acad. Sci. U. S. A.*, 2002, **99**, 19–24; (b) T. Feng, M. L. Tsao and P. G. Schultz, *J. Am. Chem. Soc.*, 2004, **126**, 15962–15963; (c) A. J. Link, M. K. S. Vink and D. A. Tirrell, *J. Am. Chem. Soc.*, 2004, **126**, 10598–10602; (d) E. M. Tookmanian, E. E. Fenlon and S. H. Brewer, *RSC Adv.*, 2015, **5**, 1274–1281.

11 W. P. Heal, B. Jovanovic, S. Bessin, M. H. Wright, A. I. Magee and E. W. Tate, *Chem. Commun.*, 2011, **47**, 4081–4083.

12 (a) T. Pathak, *Chem. Rev.*, 2002, **102**, 1623–1667; (b) A. B. Neef and N. W. Luedtke, *Chembiochem*, 2014, **15**, 789–793.

13 (a) Y. Kho, S. C. Kim, C. Jiang, D. Barma, S. W. Kwon, J. K. Cheng, J. Jaunbergs, C. Weinbaum, F. Tamanoi, J. Falck and Y. M. Zhao, *Proc. Natl. Acad. Sci. U. S. A.*, 2004, **101**, 12479–12484; (b) S. Lindner, K. Gruhle, R. Schmidt, V. M. Garamus, D. Ramsbeck, G. Hause, A. Meister, A. Sinz and S. Drescher, *Langmuir*, 2017, **33**, 4960–4973.

14 C. P. Ramil and Q. Lin, *Chem. Commun.*, 2013, **49**, 11007–11022.

15 G. Brauer, *Handbook of preparative inorganic chemistry*, Academic Press, Inc., New York, NY, 2nd edn, 1963.

16 See the detailed synthetic routes in the ESI†

17 (a) J. H. Lee, Y. Okuno and S. Cavagnero, *J. Magn. Reson.*, 2014, **241**, 18–31; (b) M. M. Chaumeil, C. Najac and S. M. Ronen, in *Methods Enzymol.*, ed. C. M. Metallo, Academic Press, 2015, vol. 561, pp. 1–71.

18 C. Y. Jao, M. Roth, R. Welti and A. Salic, *Proc. Natl. Acad. Sci. U. S. A.*, 2009, **106**, 15332–15337.

19 C. Y. Jao, M. Roth, R. Welti and A. Salic, *Chembiochem*, 2015, **16**, 472–476.

20 C. Cudalbu, A. Comment, F. Kurdzesau, R. B. van Heeswijk, K. Uffmann, S. Jannin, V. Denisov, D. Kirik and R. Gruetter, *Phys. Chem. Chem. Phys.*, 2010, **12**, 5818–5823.

21 T. B. Rodrigues, E. M. Serrao, B. W. C. Kennedy, D. E. Hu, M. I. Kettunen and K. M. Brindle, *Nat. Med.*, 2014, **20**, 93–98.

22 (a) S. T. Laughlin and C. R. Bertozzi, *Nat. Protoc.*, 2007, **2**, 2930–2944; (b) B. W. Zaro, A. R. Batt, K. N. Chuh, M. X. Navarro and M. R. Pratt, *ACS Chem. Biol.*, 2017, **12**, 787–794.

23 C. Hundhammer, M. Grashei, A. Greiner, S. J. Glaser and F. Schilling, *Chemphyschem*, 2019, **20**, 798–802.

24 (a) E. Chiavazza, A. Viale, M. Karlsson and S. Aime, *Contrast Media Mol. Imaging*, 2013, **8**, 417–421; (b) C. Hundhammer, S. Duwel, D. Ruseckas, G. Topping, P. Dzien, C. Muller, B. Feuerecker, J. B. Hovener, A. Haase, M. Schwaiger, S. J. Glaser and F. Schilling, *Sensors*, 2018, **18**, 600.

25 H. Mitsuya, K. J. Weinhold, P. A. Furman, M. H. St Clair, S. N. Lehrman, R. C. Gallo, D. Bolognesi, D. W. Barry and S. Broder, *Proc. Natl. Acad. Sci. U. S. A.*, 1985, **82**, 7096–7100.

26 (a) M. Hu, K. Roland, L. Ge, J. Chen, Y. Li, P. Tyle and S. Roy, *J. Pharm. Sci.*, 1998, **87**, 886–890; (b) T. Tahara, Z. Zhang, M. Ohno, Y. Hirao, N. Hosaka, H. Doi, M. Suzuki and H. Onoe, *EJNMMI Res.*, 2015, **5**, 45.

27 R. V. Shchepin and E. Y. Chekmenev, *J. Labelled Compd. Radiopharm.*, 2014, **57**, 621–624.

28 See the ESI† for the explanation of dependence of ¹⁴N-mediated scalar relaxation on the applied magnetic field.

